Journal of Controlled Release 383 (2025) 113826

Contents lists available at ScienceDirect

Journal of Controlled Release

journal homepage: www.elsevier.com/locate/jconrel

# Long-acting glucose-responsive insulin with swift onset-of-action

Wei Liu [a,b], Juan Zhang [a,b], Yanfang Wang [a,b], Yaqin He [a], Yuanwu Wang [a,b], Xiangqian Wei [a,b], Yuejun Yao [a,b], Jianchang Xu [a,b], Wentao Zhang [a,b], Tao Sheng [a,b], Haibin Dai [c,*], Jinqiang Wang [a,b,c,*], Zhen Gu [a,b,d,e,f,*]

[a] State Key Laboratory of Advanced Drug Delivery and Release Systems, School of Pharmacy, Zhejiang University, Hangzhou 310058, China
[b] Jinhua Institute of Zhejiang University, Jinhua 321299, China
[c] Department of Pharmacy, Second Affiliated Hospital, Zhejiang University, School of Medicine, Hangzhou 310009, China
[d] Department of General Surgery, Sir Run Run Shaw Hospital, School of Medicine, Zhejiang University, Hangzhou 310016, China
[e] Liangzhu Laboratory, Hangzhou 311121, China
[f] MOE Key Laboratory of Macromolecular Synthesis and Functionalization, Department of Polymer Science and Engineering, Zhejiang University, Hangzhou 310027, China

ARTICLE INFO

*Keywords:*
Glucose-responsive
Insulin analogs
Long-acting
Diabetes
Insulin delivery

ABSTRACT

Long-acting glucose-responsive insulin is anticipated to reduce the frequency of injections via replacing both rapid-acting and long-acting insulin. Sequential rapid glucose-responsive insulin release and instant absorption are essential to the swift onset of action. Herein, we have developed injectable long-acting glucose-responsive insulin formulations (GRIF) prepared from glucosamine-modified insulin aspart (ASP-$G_n$) and phenylboronic acid-modified poly-L-lysine (PLL-FPBA). The complex can form stable GRIF reservoir subcutaneously after injection. Upon food intake, the elevated blood glucose (BG) triggers the release of monomolecular insulin aspart (or ASP-$G_n$), which can be absorbed immediately to downregulate BG back to the normal range. Among the diverse formulations investigated, GRIF prepared from two-glucosamine-modified insulin aspart and twice weight of PLL-FPBA facilitates the best in vitro glucose-responsive insulin release performance. In type 1 diabetic mouse and minipig models, GRIF exhibit notably swift onset of action and achieve superior BG control. In addition, GRIF reveal no discernible signs of associated toxicity in the studied animals.

## 1. Introduction

Diabetes affects upwards of 537 million people worldwide, and is projected to exceed 783 million by 2045 [1]. Insulin replacement therapy is an integral part of the treatment for type 1 and advanced type 2 diabetes mellitus [2,3]. Currently, a combination of mealtime and basal insulin formulations is employed to align with the body's daily pulsatile insulin requirements heavily relied on meal intake [4]. While recombinant human insulin has traditionally been used for mealtime injections, it necessitates administration approximately 30 min before a meal and is associated with an increased risk of postprandial hypoglycemia due to delayed absorption [5,6]. Rapid-acting insulin, such as insulin aspart, can be administered immediately prior to a meal, quickly exerting its blood glucose (BG)-regulating effect as it is rapidly absorbed after injection [7–9]. In contrast, long-acting insulin, like insulin glargine, is absorbed slowly and can only meet the requirement of basal insulin [10]. Consequently, individuals with diabetes often require three to four daily injections, placing a significant burden on their daily lives [11]. An insulin formulation that can be absorbed quickly during mealtime, with gradual and slow insulin release during the fasting time, can address this issue.

In healthy individuals, the management of blood insulin levels is tightly and safely managed by $\beta$-cells, which can sense BG levels and secrete insulin rapidly during the meal and slowly during the fasting time [12,13]. To replicate this natural mechanism, various glucose-responsive insulin formulations (GRIF) have been devised utilizing glucose oxidase [14–21], phenylboronic acid [22–37], and glucose-binding molecules [38–44]. While recombinant human insulin is commonly employed in these GRIF, its slow absorption rate due to the formation of hexamers can impede the efficiency of glucose-responsive BG regulation, especially during the meal. In contrast, rapid-acting insulin, like insulin aspart, provides a rapid onset of action and shortened

* Corresponding authors at: State Key Laboratory of Advanced Drug Delivery and Release Systems, School of Pharmacy, Zhejiang University, Hangzhou 310058, China.
*E-mail addresses:* haibindai@zju.edu.cn (H. Dai), jinqiang_wang@zju.edu.cn (J. Wang), guzhen@zju.edu.cn (Z. Gu).

https://doi.org/10.1016/j.jconrel.2025.113826
Received 21 December 2024; Received in revised form 3 May 2025; Accepted 6 May 2025
Available online 8 May 2025

duration following subcutaneous injection, potentially enabling GRIF to control BG levels precisely [7,45,46]. In addition, as the incorporation of rapid-acting insulin into GRIF remains elusive, how to endow the rapid-acting insulin-integrated GRIF with superior glucose-responsive insulin release performance needs to be explored.

In this study, we have developed GRIF from positively-charged 4-carboxy-3-fluorophenylboronic acid-modified poly-*L*-lysine (PLL-FPBA) and negatively-charged insulin aspart. Insulin aspart is further modified with glucosamine (designated ASP-$G_n$) to enhance the stability of the GRIF via introducing glucose-responsive phenylboronic ester bonds between insulin (without specific notation, the term insulin indicates both ASP-$G_n$ and unmodified insulin aspart) and PLL-FPBA (Fig. 1a). Under normoglycemic conditions, insulin tightly binds to PLL-FPBA, resulting in slow insulin release to provide basal insulin for fasting BG control. Under hyperglycemic conditions, the elevated glucose concentration enhances the level of glucose binding to 4-carboxyl-3-fluorophenylboronic acid (FPBA) moieties on PLL-FPBA, triggering the dissociation of the phenylboronic ester bond and reducing the positive charge density of PLL-FPBA. This leads to decreased stability of GRIF and enhanced insulin release, thereby exerting a promoted BG-regulating effect. In streptozotocin (STZ)-induced type 1 diabetic (T1D) mice and minipigs, the GRIF composed of ASP-$G_2$ and PLL-FPBA outperforms other formulations by effectively regulating hyperglycemia and providing a BG-regulating effect for longer than one day. Importantly, GRIF exhibited a swift onset of action in comparison to insulin glargine and rapid BG-responsive insulin release in diabetic minipigs. Of note, no discernible signs of toxicity were observed in the treated animals.

## 2. Results and discussion

### 2.1. Preparation and analysis of the GRIF

PLL-FPBA was prepared from poly-*L*-lysine and FPBA (Fig. S1) [47].

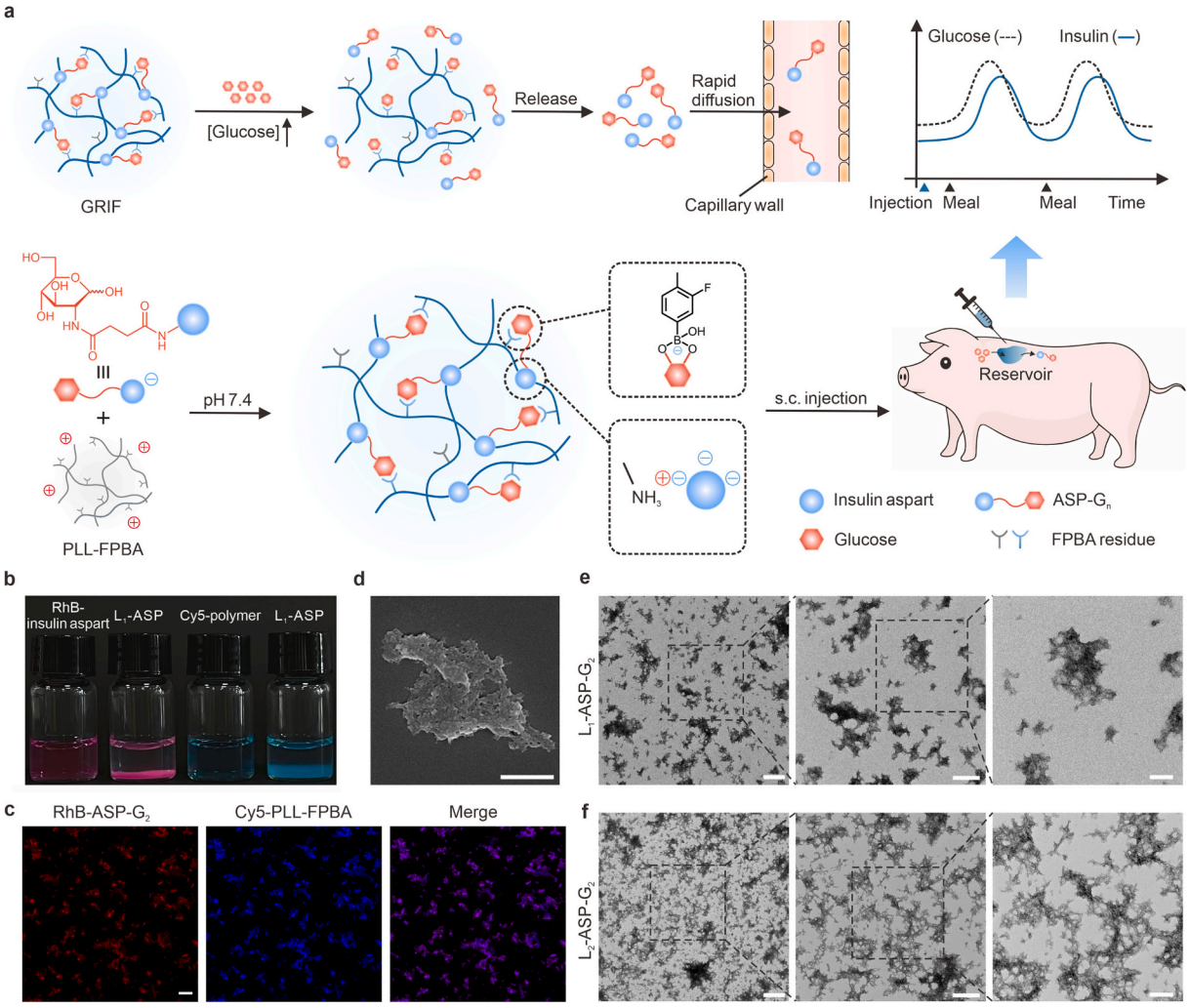


**Fig. 1.** Dual glucose-responsive insulin formulations (GRIF) for insulin analog delivery. (a) Schematic and glucose-responsive mechanism of the GRIF composed of glucosamine-modified insulin aspart (ASP-$G_n$) and phenylboronic acid-modified poly-*L*-lysine (PLL-FPBA). The formulations consist of positively charged PLL-FPBA and negatively charged ASP-$G_n$ under a physiological environment (pH = 7.4). The glucosamine moiety in ASP-$G_n$ can form reversible covalent interactions with the *cis*-diol structure in PLL-FPBA. In hyperglycemic conditions, the free glucose in the plasma and tissue competes for FPBA and decreases the positive charge of PLL-FPBA, which leads to the dissociation of ASP-$G_n$ and PLL-FPBA, and ASP-$G_n$ can rapidly normalize blood glucose (BG) levels. (b) Representative image of fluorescence-labeled GRIF. Insulin aspart and PLL-FPBA were labeled with Rhodamine B (RhB) and Cy5, respectively. RhB-insulin aspart and polymer were mixed in equal weight to obtain $L_1$-ASP shown in red, while insulin aspart and Cy5-polymer were mixed in equal weight to obtain $L_1$-ASP shown in blue. (c) Fluorescence images of GRIF ($L_1$-ASP-$G_2$). RhB-labeled ASP-$G_2$ and Cy5-labeled PLL-FPBA were shown in red and blue, respectively. Scale bar, 100 μm. (d) Representative SEM image of $L_1$-ASP-$G_2$. Scale bar, 3 μm. (e, f) Representative TEM images of $L_1$-ASP-$G_2$ (e) and $L_2$-ASP-$G_2$ (f). The GRIF images are gradually enlarged from left to right, and the scale bars are 1 μm, 0.5 μm, and 0.2 μm, respectively. (For interpretation of the references to colour in this figure legend, the reader is referred to the web version of this article.)

The chemical structure of the obtained polymer was verified by $^1$H NMR (Fig. S2). Then, glucosamine was reacted with disuccinimidyl succinate and insulin aspart sequentially to generate glucosamine-modified insulin aspart (Fig. S3). The obtained glycosylated insulin analogs were purified by liquid chromatography (Fig. S4). The obtained insulin analogs had one, two, or three glucosamine moieties and insulin analogs were named ASP-$G_1$, ASP-$G_2$, and ASP-$G_3$ accordingly (ASP: insulin aspart; $G_n$: the *n* indicated the number of glucosamine moiety in each insulin aspart analog) (Fig. S5). Their secondary structures were retained as confirmed by circular dichroism spectra (Fig. S6). Size-exclusion chromatography was used to confirm the monomeric state of modified insulin (Fig. S7). The modification sites of glucosamine to insulin aspart were further validated (Figs. S8-S10).

The GRIF were prepared via mixing acidic PLL-FPBA and ASP-$G_n$ aqueous solutions of varied ratios. After instantly modifying the pH to nearly 7.4 by NaOH aqueous solution, a flocculent precipitate formed immediately (Fig. 1b). The overlap of fluorescence of RhB-labeled ASP-$G_2$ (indicated as red) and that of Cy5-labeled PLL-FPBA (indicated as blue) confirmed the encapsulation of ASP-$G_2$ in GRIF (Fig. 1c). GRIF were micro-sized flocculent precipitates (Fig. 1d-f). This size was small enough for injection with the generally used insulin syringe. Six GRIF were obtained by varying the ratio between PLL-FPBA to ASP-$G_n$, including $L_1$-ASP-$G_1$, $L_1$-ASP-$G_2$, $L_1$-ASP-$G_3$, $L_2$-ASP-$G_1$, $L_2$-ASP-$G_2$, and $L_2$-ASP-$G_3$ ($L_1$: equal weight of PLL-FPBA to ASP-$G_n$; $L_2$: twice weight of PLL-FPBA to ASP-$G_n$).

### 2.2. *In vitro* insulin release study

The glucose-responsive insulin release ability of $L_1$-ASP, $L_2$-ASP, $L_1$-ASP-$G_1$, $L_1$-ASP-$G_2$, $L_1$-ASP-$G_3$, $L_2$-ASP-$G_1$, $L_2$-ASP-$G_2$, and $L_2$-ASP-$G_3$

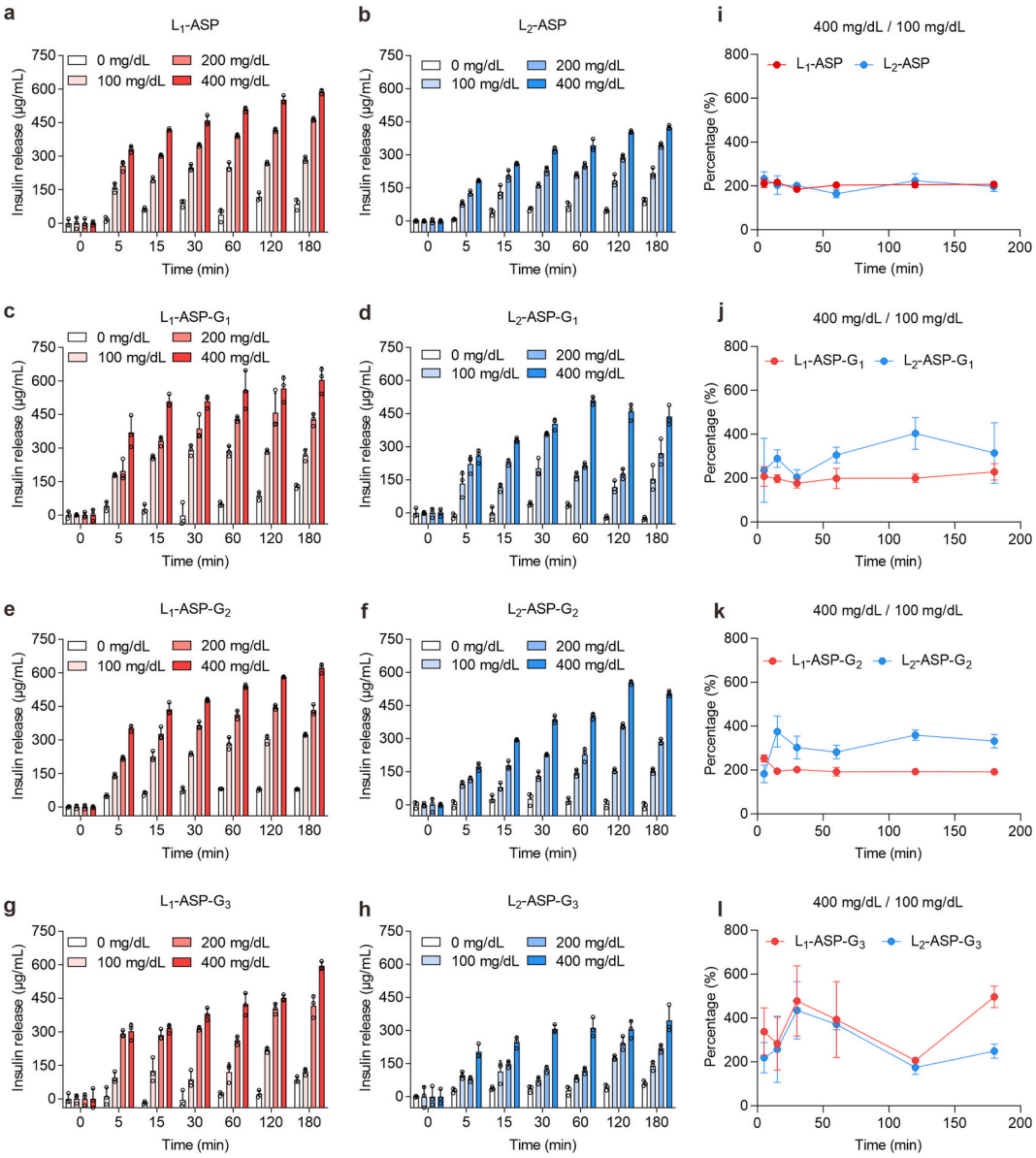


**Fig. 2.** In vitro glucose-responsive ASP-$G_n$ release. (a, b) Glucose-responsive insulin aspart release from $L_1$-ASP (a) and $L_2$-ASP (b). (c, d) Glucose-responsive ASP-$G_1$ release from $L_1$-ASP-$G_1$ (c) and $L_2$-ASP-$G_1$ (d). (e, f) Glucose-responsive ASP-$G_2$ release from $L_1$-ASP-$G_2$ (e) and $L_2$-ASP-$G_2$ (f). (g, h) Glucose-responsive ASP-$G_3$ release from $L_1$-ASP-$G_3$ (g) and $L_2$-ASP-$G_3$ (h). (i) Comparison of glucose-responsive rate when the GRIF in (a) and (b) were exposed to 100 mg/dL and 400 mg/dL glucose solution. (j) Comparison of glucose-responsive rate when the GRIF in (c) and (d) were exposed to 100 mg/dL and 400 mg/dL glucose solution. (k) Comparison of glucose-responsive rate when the GRIF in (e) and (f) were exposed to 100 mg/dL and 400 mg/dL glucose solution. (l) Comparison of glucose-responsive rate when the GRIF in (g) and (h) were exposed to 100 mg/dL and 400 mg/dL glucose solution. Data are presented as means ± SD ($n = 3$).

was evaluated in vitro. Standard curves of insulin aspart and ASP-$G_n$ were established by using the Bradford assay reagent (Fig. S11). In PBS solution (pH = 7.4), PLL-FPBA was virtually insoluble, showing essentially no background signal (Fig. S12). The encapsulation efficiency of insulin aspart and ASP-$G_n$ in all GRIF was above 85 % (Fig. S13). The insulin aspart release of the GRIF was assessed in PBS (pH = 7.4) with glucose (0, 100, 200, and 400 mg/dL). Insulin aspart release from all GRIF can be accelerated after the introduction of glucose. At 0 mg/dL glucose solution, free insulin aspart concentrations in $L_1$-ASP and $L_2$-ASP groups were equilibrated at concentrations of 85.6 ± 24.4 and 92.0 ± 12.5 μg/mL in 180 min, respectively (Fig. 2a, b). In the normoglycemia-mimicking group (100 mg/dL glucose solution), the mild-hyperglycemia-mimicking group (200 mg/dL glucose solution), and the extreme hyperglycemia-mimicking group (400 mg/dL glucose solution), the insulin aspart release rates were all accelerated and equilibrium concentrations reached 284.5 ± 11.3 and 217.2 ± 22.5 μg/mL, 464.4 ± 6.0 and 343.7 ± 9.5 μg/mL, and 588.5 ± 10.0 and 424.7 ± 8.5 μg/mL, respectively, after three hours' incubation. Compared with $L_1$-ASP and $L_2$-ASP, $L_1$-ASP-$G_1$, $L_1$-ASP-$G_2$, $L_1$-ASP-$G_3$, $L_2$-ASP-$G_1$, $L_2$-ASP-$G_2$, and $L_2$-ASP-$G_3$ included the reversible binding of FPBA to the *cis*-diol structure of glucosamine residues (Fig. 2c-h). After 180 min incubation in the 100 mg/dL glucose solution, free insulin aspart reached equilibrium concentrations of 267.3 ± 24.8, 323.5 ± 3.9, 120.8 ± 14.0, 154.9 ± 56.5, 152.8 ± 11.5, and 139.2 ± 20.2 μg/mL for $L_1$-ASP-$G_1$, $L_1$-ASP-$G_2$, $L_1$-ASP-$G_3$, $L_2$-ASP-$G_1$, $L_2$-ASP-$G_2$, and $L_2$-ASP-$G_3$, respectively. In the 200 mg/dL glucose solution, the equilibrium concentrations of ASP-$G_n$ reached 426.8 ± 26.6, 433.0 ± 22.6, 416.8 ± 48.6, 271.3 ± 59.1, 286.1 ± 11.1, and 217.9 ± 16.9 μg/mL in $L_1$-ASP-$G_1$, $L_1$-ASP-$G_2$, $L_1$-ASP-$G_3$, $L_2$-ASP-$G_1$, $L_2$-ASP-$G_2$, and $L_2$-ASP-$G_3$, respectively. Further increasing glucose concentration to 400 mg/dL, the equilibrium concentrations reached 605.0 ± 56.9, 619.8 ± 19.4, 595.3 ± 18.4, 437 ± 45.7, 504.3 ± 11.5, and 345.8 ± 63.1 μg/mL after 180 min incubation in $L_1$-ASP-$G_1$, $L_1$-ASP-$G_2$, $L_1$-ASP-$G_3$, $L_2$-ASP-$G_1$, $L_2$-ASP-$G_2$, and $L_2$-ASP-$G_3$, respectively.

Compared to GRIF prepared from insulin aspart, glucosamine-modified GRIF exhibited similar or reduced equilibrium concentrations under normoglycemic conditions but similar or even higher equilibrium insulin concentrations under hyperglycemic conditions. The introduction of phenylboronic ester bonds enhanced the stability of GRIF, therefore reducing the equilibrium concentration of insulin. Under hyperglycemia conditions, glucose bonding to FPBA residues in PLL-FPBA reversed the positive charge, and cleaved the phenylboronic ester bond between PLL-FPBA and ASP-$G_n$, therefore leading to the dissociation of ASP-$G_n$ and PLL-FPBA and elevating the equilibrium ASP-$G_n$ concentration. The glucose stimulation index (GSI) defined as the ratio of the insulin release rate from GRIF at varied glucose conditions was then calculated. $GSI_4$ and $GSI_2$ were defined as the ratio of the insulin concentration in 400 and 200 mg/dL glucose solutions to the insulin concentration in 100 mg/dL glucose solution, respectively. All GRIF showed $GSI_2$ for around 200 % (Fig. S14). Both $L_1$-ASP and $L_2$-ASP exhibited $GSI_4$ of around 200 % (Fig. 2i). As a comparison, $GSI_4$ can be as high as 400 % at specific time points for all $L_n$-ASP-$G_n$ (Fig. 2j-l). Especially, $L_2$-ASP-$G_2$ exhibited a stable $GSI_4$ near 400 % (Fig. 2k).

### 2.3. *In vivo* treatment study in T1D mouse model

The BG management capability of insulin aspart, ASP-$G_n$, and the prepared GRIF was evaluated in STZ-induced T1D mice (BG level above 300 mg/dL). After subcutaneous injection with insulin aspart or ASP-$G_n$ at a dose of 1.5 mg/kg, the BG of all treated mice normalized below 200 mg/dL within 30 min and maintained below 200 mg/dL for around 2 h, indicating no significant difference in their bioactivity (Fig. 3a). Two commercially available long-acting insulins, including insulin glargine (40 U/kg) and insulin detemir (40 U/kg), were also evaluated. A single injection of insulin glargine and insulin detemir can bring BG to 130.0 ± 29.0 and 168.1 ± 36.9 mg/dL in about 30 min, and this glycemic control can be maintained for about 9 h (Fig. 3b and S15a). Then, T1D mice were treated with GRIF at a dose of 1.5 mg/kg (Fig. 3c, d). After treated with $L_1$-ASP, $L_1$-ASP-$G_1$, $L_1$-ASP-$G_2$, and $L_1$-ASP-$G_3$, the BG of mice decreased to 195.1 ± 57.2, 152.6 ± 71.9, 142.2 ± 30.0, and 160.6 ± 31.5 mg/dL within 15 min, to 123.8 ± 19.2, 124.2 ± 42.4, 115.6 ± 24.8, and 129.2 ± 13.8 mg/dL in 30 min, and maintained at a normal range (below 200 mg/dL) for 8.9 ± 1.1, 10.9 ± 1.8, 13.0 ± 1.8, and 11.4 ± 1.7 h, respectively (Fig. 3c and S15b). As a comparison, a single

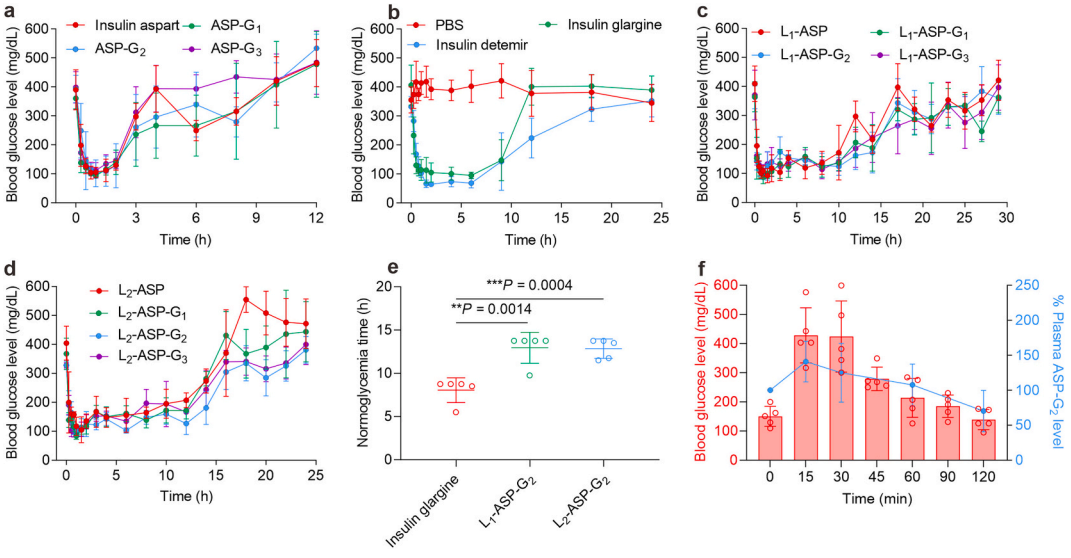


**Fig. 3.** Evaluation of GRIF in type 1 diabetic (T1D) mice. (a) BG of STZ-induced T1D mice treated with insulin aspart and ASP-$G_n$ at 1.5 mg/kg. Data are presented as means ± SD ($n$ = 6). (b) BG levels of T1D mice treated with PBS, insulin glargine, and insulin detemir. The dose of insulin glargine and insulin detemir was 40 U/kg. Data are presented as means ± SD ($n$ = 5). (c) BG levels of T1D mice treated with $L_1$-ASP, $L_1$-ASP-$G_1$, $L_1$-ASP-$G_2$, and $L_1$-ASP-$G_3$ with the same dose (1.5 mg/kg). Data are presented as means ± SD ($n$ = 5). (d) BG levels of T1D mice treated with $L_2$-ASP, $L_2$-ASP-$G_1$, $L_2$-ASP-$G_2$, and $L_2$-ASP-$G_3$ with the same dose (1.5 mg/kg). Data are presented as means ± SD ($n$ = 5). (e) Normoglycemic time of T1D mice treated with insulin glargine, $L_1$-ASP-$G_2$, and $L_2$-ASP-$G_2$. Data are presented as means ± SD ($n$ = 5). Unpaired $t$-test (two-tailed) was used for statistical analysis. The normoglycemia is defined as BG between 50 and 200 mg/dL. (f) BG levels and plasma ASP-$G_2$ levels after intraperitoneal glucose injection (3.0 g/kg). Diabetic mice were treated with $L_2$-ASP-$G_2$ (1.5 mg/kg). Data are presented as means ± SD ($n$ = 5).

subcutaneous injection of $L_2$-ASP, $L_2$-ASP-$G_1$, $L_2$-ASP-$G_2$, and $L_2$-ASP-$G_3$ regulated BG of mice from hyperglycemia to 199.8 ± 105.4, 138.6 ± 25.8, 198.0 ± 42.6, and 190.8 ± 33.2 mg/dL within 15 min, to 160.2 ± 23.6, 142.9 ± 21.7, 164.9 ± 37.5, and 103.3 ± 21.4 mg/dL within 30 min, and maintained BG below 200 mg/dL for 9.3 ± 2.6, 10.6 ± 1.8, 12.9 ± 1.1, and 11.2 ± 3.3 h, respectively (Fig. 3d and S15c). All GRIF showed smooth BG levels with no severe hypoglycemia condition (below 50 mg/dL) observed. Among all GRIF, $L_1$-ASP-$G_2$ and $L_2$-ASP-$G_2$ showed the longest BG control ability, even slightly longer than commercially available insulin glargine (Fig. 3e).

Thus, the glucose-responsive insulin-releasing behavior of $L_2$-ASP-$G_2$ was further explored by an intraperitoneal glucose tolerance test. T1D mice were given subcutaneous injection with $L_2$-ASP-$G_2$ (1.5 mg/kg), and treated with glucose solution (3.0 g/kg) at 6 h after administration. The initial average BG level of diabetic mice was 150.5 ± 34.1 mg/dL (Fig. 3f). Then, the BG levels increased after glucose administration, peaked at 428.4 ± 94.5 mg/dL at 15 min, and returned to the initial level within 120 min, with similar BG control capability as in healthy mice (Fig. 3f and S16a). Of note, an increase in plasma insulin level was observed along with the increase in BG (Fig. 3f). T1D mice with PBS or insulin aspart (1.5 mg/kg) for 6 h did not restore normoglycemia nor produce glucose-responsive insulin fluctuations for 120 min after glucose injection (Fig. S16b, c and S17).

### 2.4. In vivo treatment study in T1D minipig model

Because $L_2$-ASP-$G_2$ showed glucose-triggered insulin release and exhibited a longer duration of action than insulin glargine, $L_2$-ASP-$G_2$ was thus further selected to treat T1D minipigs. T1D Bama minipigs were induced by intravenous injection of STZ. Minipigs with BG levels above 200 mg/dL were selected. The diabetic minipigs were fed twice daily, and insulin glargine was generally used for BG control. The BG was monitored using continuous glucose monitoring system (CGMS) affixed to the legs of minipigs. In the absence of treatment, the BG level of three minipigs was mainly maintained above 200 mg/dL and fluctuated due to the circadian rhythm and feeding (Fig. 4a-c). Minipigs were then administered with insulin glargine or $L_2$-ASP-$G_2$ with a gap of two days after the daily insulin glargine treatment. These minipigs were administered subcutaneously with insulin glargine at 0.40, 0.35, and 0.40 U/kg for pig#1, pig#2 and pig#3, respectively (Fig. 4a-c). Also, these minipigs were injected subcutaneously with $L_2$-ASP-$G_2$ at 0.07, 0.06, and 0.07 mg/kg (Fig. 4a-c). BG levels of insulin glargine-treated and $L_2$-ASP-$G_2$-treated minipigs decreased to below 200 mg/dL in 4.5 ± 0.9 and 0.9 ± 0.1 h, respectively (Fig. 4d). In the $L_2$-ASP-$G_2$-treated group, BG within the normal range (50 to 200 mg/dL) occupied 54.9 ± 13.9 % of monitoring time, which is 1.5 times longer than that of minipigs administered with insulin glargine (Fig. 4e). Since the lower detection limit of CGMS was 40 mg/dL, BG between 40 and 50 mg/dL was defined as the hypoglycemic range. No significant difference in hypoglycemia risk was identified between groups treated with insulin glargine and $L_2$-ASP-$G_2$ (Fig. 4e). Healthy minipig maintained BG between 40 and 60 mg/dL, with BG at or below the lower limit of detection of CGMS sometimes observed (Fig. S18). The minipigs treated with $L_2$-ASP-$G_2$ and insulin glargine did not show symptoms associated with hypoglycemia during treatment. In vivo glucose tolerance test was performed 5 h after subcutaneous injection of $L_2$-ASP-$G_2$ at doses of 0.07, 0.06, and 0.07 mg/kg, respectively. Rapid serum ASP-$G_2$ release was observed and BG was able to return to normal range within 30 min after intravenous glucose infusion (Fig. 4f).

### 2.5. In vivo toxicity and biocompatibility of the GRIF

Hematoxylin and eosin (H&E) staining and Masson's Trichrome staining were then used to explore the residence time and host response of $L_2$-ASP-$G_2$ (1.5 mg/kg) after subcutaneous injection. No significant fibrous capsule and neutrophil infiltration were observed in H&E staining and Masson's Trichrome staining one day, one week, and three months after administration of $L_2$-ASP-$G_2$ (Fig. 5a, b). Importantly, the depot was completely cleared from the injection sites after 12 weeks (Fig. 5a, b). Moreover, $L_2$-ASP and $L_2$-ASP-$G_2$ displayed negligible impacts on serum biochemical parameters and cell counts of the treated mice (Fig. 5c, d).

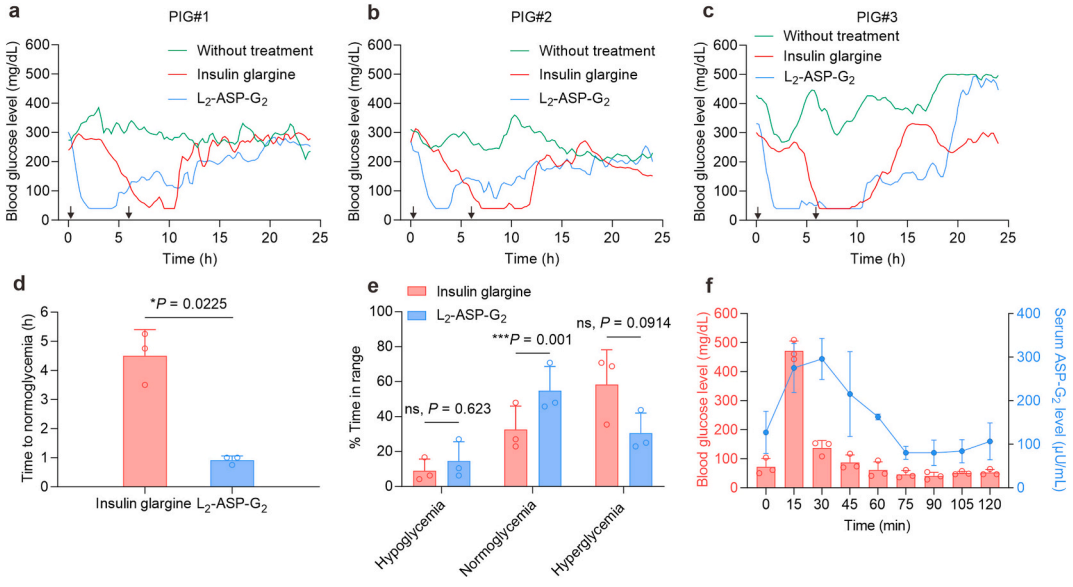


**Fig. 4.** Evaluation of GRIF in T1D minipigs. (a-c) BG of diabetic minipigs treated with $L_2$-ASP-$G_2$ and insulin glargine. The dose of insulin glargine was set to 0.40, 0.35 and 0.40 U/kg for pig#1, pig#2 and pig#3, respectively. The dose of $L_2$-ASP-$G_2$ was set to 0.07, 0.06, and 0.07 mg/kg for pig#1, pig#2 and pig#3, respectively. BG was monitored by continuous glucose monitoring system. Arrows indicate the feeding of minipig. (d) Time required for subcutaneously injected insulin glargine and $L_2$-ASP-$G_2$ to regulate BG toward 200 mg/dL. Data are presented as means ± SD ($n = 3$). (e) Time of hypoglycemia (BG < 50 mg/dL), normoglycemia (BG range 50 to 200 mg/dL) and hyperglycemia (BG > 200 mg/dL) in 24 h after subcutaneous injection of insulin glargine and $L_2$-ASP-$G_2$. Data are presented as means ± SD ($n = 3$). (f) The serum insulin level changed after glucose infusion for 15 min at a rate of 1 L/h. Data are presented as means ± SD ($n = 3$). Paired *t*-test (two-tailed) was used for statistical analysis.

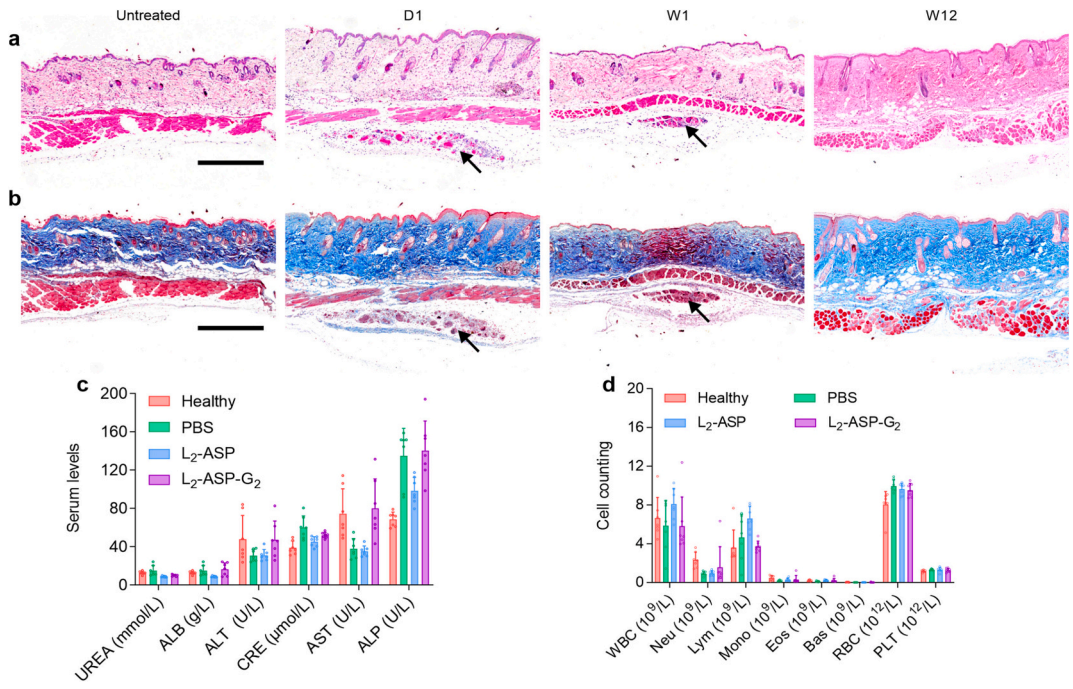


**Fig. 5.** The biocompatibility of GRIF. (a, b) Representative images of H&E staining (a) and Masson's trichrome staining (b) sections. Mice were subcutaneously injected with the same dosage of $L_2$-ASP-$G_2$ (1.5 mg/kg). The black arrows represent the subcutaneously retained GRIF. Scale bars, 500 μm. (c) The effect of GRIF on biochemical parameters in mice serum. PBS, $L_2$-ASP, and $L_2$-ASP-$G_2$ were administered subcutaneously to mice once daily for one week at a dose of 1.5 mg/kg. Healthy mice were selected as the control group. One week later, serum was extracted using serum separator tube after clotting the blood for 30 min. Data are presented as means ± SD ($n = 7$). ALB, albumin; ALT, alanine transaminase; CRE, creatinine; AST, aspartate transaminase; ALP, alkaline phosphatase. (d) The effect of the GRIF on cell counts in mice blood. PBS, $L_2$-ASP, and $L_2$-ASP-$G_2$ were administered subcutaneously to mice once daily for 1 week at a dose of 1.5 mg/kg. Healthy mice were selected as the control group. One week later, the whole blood was collected through orbital blood sampling. Data are presented as means ± SD ($n = 7$). WBC, white blood cell; Neu, neutrophil; Lym, lymphocyte; Mono, monocyte; Eos, eosinophil; Bas, basophil; RBC, red blood cell; PLT, platelet. (For interpretation of the references to colour in this figure legend, the reader is referred to the web version of this article.)

## 3. Conclusions

In this work, we have prepared GRIF from glucosamine-modified insulin aspart and glucose-responsive cationic polymeric carrier PLL-FPBA. GRIF can effectively prolong the duration of action through electrostatic and covalent interactions. By introducing diol groups onto insulin aspart, GRIF showed robust glucose-responsive capability while retaining the rapid glucose-lowering effect of insulin aspart. Among the investigated GRIF, $L_2$-ASP-$G_2$ showed the optimal glucose responsiveness among GRIF concerning the ratio of equilibrium insulin levels in 400 mg/dL glucose solution to equilibrium insulin levels in 100 mg/dL glucose solution. In the T1D mouse model, GRIF, including $L_1$-ASP, $L_1$-ASP-$G_1$, $L_1$-ASP-$G_2$, $L_1$-ASP-$G_3$, $L_2$-ASP, $L_2$-ASP-$G_1$, $L_2$-ASP-$G_2$, and $L_2$-ASP-$G_3$, exhibited prolonged BG-regulating compared with insulin glargine and insulin detemir. Especially, $L_1$-ASP-$G_2$ and $L_2$-ASP-$G_2$ exhibited normoglycemia duration exceeding 13 h. In T1D minipigs, $L_2$-ASP-$G_2$ exhibited longer maintenance of normoglycemia and shorter onset of action compared to insulin glargine. In addition, robust and clear glucose-triggered insulin release has been identified in mice and minipigs, confirming its inner glucose-responsive character. Glucose-responsive insulin release, fast onset of action, and prolonged duration all suggest that $L_2$-ASP-$G_2$ is a potential candidate for all-in-one long-acting insulin that can replace both the current long-acting basal insulin and fast-acting insulin.

## 4. Material and methods

### 4.1. Experimental reagents

4-Carboxy-3-fluorophenylboronic acid was procured from Aladdin. Poly-ʟ-lysine (molecular weight of 30,000-70,000 kg/mol) was procured from Sigma-Aldrich. Recombinant human insulin was procured from Solarbio. Insulin aspart was purchased from Nanjing Hanxin. Streptozotocin (STZ) was purchased from Macklin. Coomassie Plus Protein Assay Reagent was purchased from Bio-Rad. Human insulin ELISA kit was purchased from Elabscience. FPBA-NHS and PLL-FPBA were prepared according to the literature [47]. Other reagents or organic solvents were purchased from Aladdin unless mentioned.

### 4.2. Synthesis of ASP-$G_n$

Disuccinimidyl succinate (50 mg) and glucosamine (35 mg) were dissolved in DMF (10 mL), with subsequent addition of triethylamine (80 μL). After 3 h reaction at room temperature, DMF was removed under reduced pressure and deionized water (10 mL) was added. After centrifugation, the supernatant was gathered and the precipitate was discarded. Insulin aspart (50 mg) dissolved in PBS (0.01 M, pH = 7.4, 10 mL) was subsequently added to the collected supernatant. The reaction was carried out for 12 h at 4 °C. Then, the mixture was dialyzed in 4 × 4 L deionized water. The obtained aqueous solution was lyophilized to obtain a white powder. The compounds were purified by preparative liquid chromatography to provide the insulin derivatives. The obtained pure glucosamine-modified insulin aspart compounds were characterized by MALDI-TOF MS.

### 4.3. Characterization of ASP-$G_n$

ASP-$G_n$ and DL-dithiothreitol (10 mmol/L) were dissolved in deionized water, and reduced in a water bath at 56 °C for 1 h. Iodoacetamide solution (50 mmol/L) was added and reacted for 40 min in the dark. Trypsin was added and the reaction was carried out at 37 °C overnight. After digestion, the peptides were desalted using a self-

priming desalting column, and the solvent was evaporated in a vacuum centrifuge at 45 °C. The peptides were dissolved in the sample solvent (0.1 % formic acid, 2 % acetonitrile), vortexed and centrifuged, and the supernatant was characterized by Nano LC-MS/MS (Easy-nLC 1200 system coupled with a Q Exactive™ Hybrid Quadrupole-Orbitrap™ Mass Spectrometer). The raw MS files were analyzed using Byonic and searched in protein databases.

For size-exclusion chromatography, a chromatographic column (PreCot Super Tandex 75 pg, 5 mL) was selected to analyze the samples, while 20 mM phosphate buffer at pH 7.4 was used as the mobile phase. The column was pre-equilibrated at 25 °C with a flow rate of 0.5 mL/min. Insulin aspart and modified-insulin aspart were dissolved in zinc-containing or zinc-free buffer (1 mg/mL, and incubated at room temperature for 1 h). After centrifugation and filtration, the samples (500 μL) were injected and measured with a UV detector at the wavelength of 280 nm. The retention times of each compound before and after zinc ion treatment were comparable with each other.

### 4.4. Preparation of GRIF, with $L_1$-ASP as an example

Either insulin aspart (10 mg) or PLL-FPBA (10 mg) was added into deionized water (1 mL), to which HCl aqueous solution (1 mol/L, 15 μL) was introduced to regulate the pH to approximately 3–4. 100 μL of each solution was mixed in an EP tube. One drop of 1 mol/L NaOH solution was then introduced to regulate the pH to 7.4. After centrifugation, the supernatant was extracted and the precipitate was resuspended by adding PBS (0.01 M, pH = 7.4, 1 mL). The concentration was adjusted to an insulin-aspart equivalent of 1 mg/mL.

### 4.5. Preparation of fluorescence-labeled ASP-$G_n$ and PLL-FPBA

ASP-$G_n$ (20 mg) was dissolved in $NaHCO_3$ (0.1 mol/L, 2 mL), to which Rhodamine B isocyanate (2 mg) dissolved in DMSO (200 μL) was added dropwise. After an overnight reaction at room temperature, the mixture was dialyzed in 4 × 4 L deionized water, and the product was freeze-dried to obtain a red powder. Cy5-PLL-FPBA was synthesized similarly.

### 4.6. Characterization of GRIF

The GRIF were suspended in deionized water at an ASP-$G_n$ concentration of 0.5 mg/mL. The GRIF were deposited onto a copper grid and kept for 1 min before being removed by a filter paper. Phosphotungstic acid solution (2 wt%) was added for 1 min before using filter paper to absorb the solution. The samples were then left to dry naturally at room temperature. The GRIF were observed by TEM (Talos L120C, Thermo Scientific). For SEM observation, the GRIF were dropped onto the silicon wafer and dried naturally at room temperature, then observed under SEM (Nova Nano 450, Thermo Scientific). The GRIF with RhB-ASP-$G_n$ and Cy5-PLL-FPBA were added dropwise to a confocal dish, and then confocal morphology (LSM 800 with Airyscan, ZEISS) of the GRIF was observed.

### 4.7. In vitro insulin analog release study

The GRIF were prepared at an ASP-$G_n$-equivalent concentration of 1 mg/mL in PBS (0.01 M, pH = 7.4, 1 mL). Then, glucose solution (0.4 g/mL) was introduced into the suspension to obtain different initial glucose concentrations (0, 100, 200, and 400 mg/dL) and cultured at 37 °C. At 0, 5, 15, 30, 60, 120, and 180 min, 50 μL of the GRIF suspension was obtained and centrifuged. Then, 10 μL of the supernatant was mixed with 200 μL of Coomassie Brilliant Blue. The absorbance of the mixture at 595 nm was quantified using a microplate reader. The encapsulation efficiency of the GRIF was derived by calculating the concentration of ASP-$G_n$ in the liquid above the precipitate using an established standard curve. PLL-FPBA was suspended in PBS (0.01 M, pH = 7.4, 1 mL) containing glucose concentrations (0, 100, 200, and 400 mg/dL). The suspension was incubated at 37 °C for 1 h, after which the supernatant was collected and assayed for apparent insulin release using Coomassie Brilliant Blue.

### 4.8. In vivo treatment efficacy in T1D mice

All laboratory animal operations were approved by the Laboratory Animal Welfare and Ethics Review Committee of Zhejiang University and conducted by the Guidelines for the Care and Use of Laboratory Animals of Zhejiang University (Protocol No. ZJU20220493). Male C57BL/6 mice were procured from Hangzhou Medical College. T1D mice were triggered by intraperitoneal injection of STZ (120 mg/kg). In assessing the BG regulatory capacity of GRIF, mice were provided with a standard diet and placed in a 12-h light and 12-h dark cycle. Mice with random BG levels between 300 and 600 mg/dL were selected and grouped. GRIF were prepared into suspensions with an ASP-$G_n$ equivalent concentration of 1 mg/mL and were administered at a dose of 1.5 mg/kg. BG levels were measured (Aviva, ACCU-CHEK) after administration until BG levels were restored to the original hyperglycemic condition.

### 4.9. Intraperitoneal glucose tolerance test in T1D mice

T1D mice were randomized and injected subcutaneously with various GRIF (1.5 mg/kg, $n = 5$). At 6 h after administration, treated mice were intraperitoneally injected with glucose (3.0 g/kg). The BG levels were measured (Aviva, ACCU-CHEK) before and after intraperitoneal injection of glucose, and blood specimens (40 μL) were gathered at 0, 15, 30, 60, and 120 min for blood plasma extraction. Plasma insulin levels were determined using a human insulin ELISA kit (Elabscience). Healthy mice ($n = 5$), PBS and insulin-aspart-treated T1D mice ($n = 5$) were used as controls. For the control groups, 3.0 g/kg of glucose solution was injected intraperitoneally after 6 h of administration. BG levels were recorded at 0, 15, 30, 45, 60, 90, and 120 min. For the PBS-treated group, plasma insulin levels were determined using a human insulin ELISA kit (Elabscience).

### 4.10. In vivo treatment efficacy study in T1D minipigs

The minipigs were acquired from Shanghai Jiagan Biotechnology Company. The minipigs were kept in a single cage with regular and quantitative feed and free water. T1D minipigs were induced by intravenously injected STZ (120 mg/kg). Minipigs received two feedings daily. When not receiving treatment, insulin glargine was injected once daily. Insulin glargine was withheld for 48 h prior to administration. Minipigs 1, 2, and 3 received subcutaneous injections of insulin glargine (0.40, 0.35 and 0.40 U/kg) and $L_2$-ASP-$G_2$ (0.07, 0.06 and 0.07 mg/kg), then CGMS (FreeStyle Libre, Abbott) was used to monitor the BG levels.

### 4.11. Glucose tolerance test in T1D minipigs

T1D minipigs 1, 2, and 3 received subcutaneous injections of $L_2$-ASP-$G_2$ at doses of 0.07, 0.06, and 0.07 mg/kg, respectively. Five hours post-administration of GRIF, minipigs were anaesthetized using isoflurane. The glucose solution (5 wt%) was infused intravenously for 15 min at a rate of 1 L/h. The BG of minipigs rose rapidly to more than 300 mg/dL, and the infusion was stopped. The blood sample was extracted from the jugular vein before and every 15 min for 2 h after the glucose infusion. Blood samples (2 mL) were collected in anticoagulation tubes (BD Vacutainer) and left to clot naturally for 30 min at room temperature. The sample was centrifuged (1500 G, 10 min) so that the serum and the blood clot were completely separated by the separating gel. Serum insulin concentrations were determined using a human insulin ELISA kit (Elabscience).

### 4.12. Biocompatibility assessment in T1D mice

$L_2$-ASP-$G_2$ was prepared with Cy5-labeled PLL-FPBA. T1D mice were subcutaneously injected with $L_2$-ASP-$G_2$ (1.5 mg/kg). One day, one week, and 12 weeks later, skin tissues containing $L_2$-ASP-$G_2$ were cut from euthanized mice for H&E and Masson's trichrome staining. Mice were injected subcutaneously with PBS, $L_2$-ASP, and $L_2$-ASP-$G_2$ with an insulin aspart-equivalent dose of 1.5 mg/kg once daily for one week. One week later, whole blood was collected and serum was extracted for physiological and biochemical parameters.

### 4.13. Statistical analysis

Statistical significance in all figures was calculated by a two-tailed Student's *t*-test. $^{*}P < 0.05$, $^{**}P < 0.01$, $^{***}P < 0.001$, $^{****}P < 0.0001$, ns, not significant. All *P*-value analyses were performed on GraphPad Prism 8.

## CRediT authorship contribution statement

**Wei Liu:** Writing – review & editing, Writing – original draft, Visualization, Methodology, Investigation. **Juan Zhang:** Writing – review & editing, Investigation. **Yanfang Wang:** Writing – review & editing, Investigation. **Yaqin He:** Writing – review & editing, Investigation. **Yuanwu Wang:** Writing – review & editing. **Xiangqian Wei:** Investigation. **Yuejun Yao:** Writing – review & editing, Investigation. **Jianchang Xu:** Writing – review & editing, Investigation. **Wentao Zhang:** Investigation. **Tao Sheng:** Investigation. **Haibin Dai:** Supervision, Conceptualization. **Jinqiang Wang:** Writing – review & editing, Supervision, Conceptualization. **Zhen Gu:** Writing – review & editing, Supervision, Conceptualization.

## Declaration of competing interest

Z.G. is the co-founder of Zenomics Inc., Zcapsule Inc., and $\mu$Zen Inc.. The other authors declaim no conflict of interests.

## Acknowledgements

This work was supported by the grants from National Key Research and Development Program of China (2022YFE0202200), Key R&D Program of Zhejiang Province (2024C03085, J.W.), National Natural Science Foundation of China (32471374, J.W.), and JDRF (2-SRA-2021-1064-M-B, 2-SRA-2022-1159-M-B). We are grateful for the assistance provided by Guizhen Zhu and Yuchen Zhang (Cryo-EM Centre, Zhejiang University) in preparing samples for electron microscopy, Jianyang Pan and Dan Wu (Research and Service Center, College of Pharmaceutical Science, Zhejiang University), Chao Sun and Huiwen Wang (Analysis Center of Agrobiology and Environmental Sciences, Zhejiang University) for MALDI-TOF mass spectrometry analysis, Deyue Xu (Animal Center, Zhejiang University) for tending to minipigs, Danjing Guo (Division of Hepatobiliary and Pancreatic Surgery, Department of Surgery, The First Affiliated Hospital, Zhejiang University School of Medicine) for sectioning and staining skin tissue.

## Appendix A. Supplementary data

Supplementary data to this article can be found online at https://doi.org/10.1016/j.jconrel.2025.113826.

## Data availability

Data will be made available on request.

## References

[1] H. Sun, P. Saeedi, S. Karuranga, M. Pinkepank, K. Ogurtsova, B.B. Duncan, C. Stein, A. Basit, J.C.N. Chan, J.C. Mbanya, M.E. Pavkov, A. Ramachandaran, S.H. Wild, S. James, W.H. Herman, P. Zhang, C. Bommer, S. Kuo, E.J. Boyko, D.J. Magliano, IDF diabetes atlas: global, regional and country-level diabetes prevalence estimates for 2021 and projections for 2045, Diabetes Res. Clin. Pract. 183 (2022) 109119.
[2] C. Mathieu, P.J. Martens, R. Vangoitsenhoven, One hundred years of insulin therapy, Nat. Rev. Endocrinol. 17 (12) (2021) 715–725.
[3] J.B. Cole, J.C. Florez, Genetics of diabetes mellitus and diabetes complications, Nat. Rev. Nephrol. 16 (7) (2020) 377–390.
[4] K.J. Bell, B.R. King, A. Shafat, C.E. Smart, The relationship between carbohydrate and the mealtime insulin dose in type 1 diabetes, J. Diabetes Complicat. 29 (8) (2015) 1323–1329.
[5] J. Gumprecht, K. Nabrdalik, Hypoglycemia in patients with insulin-treated diabetes, Pol. Arch. Med. Wewn. 126 (11) (2016) 870–878.
[6] J. Kaur, E.R. Seaquist, Hypoglycaemia in type 1 diabetes mellitus: risks and practical prevention strategies, Nat. Rev. Endocrinol. 19 (3) (2023) 177–186.
[7] C. Mathieu, P. Gillard, K. Benhalima, Insulin analogues in type 1 diabetes mellitus: getting better all the time, Nat. Rev. Endocrinol. 13 (7) (2017) 385–399.
[8] D. Owens, J. Vora, Insulin aspart: a review, Expert Opin. Drug Metab. Toxicol. 2 (5) (2006) 793–804.
[9] K. Hermansen, M. Bohl, A.G. Schioldan, Insulin Aspart in the Management of Diabetes Mellitus: 15 years of clinical experience, Drugs 76 (1) (2016) 41–74.
[10] R.K. Campbell, J.R. White, T. Levien, D. Baker, Insulin glargine, Clin. Ther. 23 (12) (2001) 1938–1957 (discussion 1923).
[11] A.N. Zaykov, J.P. Mayer, R.D. DiMarchi, Pursuit of a perfect insulin, Nat. Rev. Drug Discov. 15 (6) (2016) 425–439.
[12] J.E. Campbell, C.B. Newgard, Mechanisms controlling pancreatic islet cell function in insulin secretion, Nat. Rev. Mol. Cell Biol. 22 (2) (2021) 142–158.
[13] D.L. Eizirik, L. Pasquali, M. Cnop, Pancreatic β-cells in type 1 and type 2 diabetes mellitus: different pathways to failure, Nat. Rev. Endocrinol. 16 (7) (2020) 349–362.
[14] J. Yu, Y. Zhang, Y. Ye, R. DiSanto, W. Sun, D. Ranson, F.S. Ligler, J.B. Buse, Z. Gu, Microneedle-array patches loaded with hypoxia-sensitive vesicles provide fast glucose-responsive insulin delivery, Proc. Natl. Acad. Sci. USA 112 (27) (2015) 8260–8265.
[15] Z. Chen, J. Wang, W. Sun, E. Archibong, A.R. Kahkoska, X. Zhang, Y. Lu, F.S. Ligler, J.B. Buse, Z. Gu, Synthetic beta cells for fusion-mediated dynamic insulin secretion, Nat. Chem. Biol. 14 (1) (2018) 86–93.
[16] Z. Gu, T.T. Dang, M. Ma, B.C. Tang, H. Cheng, S. Jiang, Y. Dong, Y. Zhang, D. G. Anderson, Glucose-responsive microgels integrated with enzyme nanocapsules for closed-loop insulin delivery, ACS Nano 7 (8) (2013) 6758–6766.
[17] Z. Gu, A.A. Aimetti, Q. Wang, T.T. Dang, Y. Zhang, O. Veiseh, H. Cheng, R. S. Langer, D.G. Anderson, Injectable nano-network for glucose-mediated insulin delivery, ACS Nano 7 (5) (2013) 4194–4201.
[18] J. Yu, C. Qian, Y. Zhang, Z. Cui, Y. Zhu, Q. Shen, F.S. Ligler, J.B. Buse, Z. Gu, Hypoxia and $H_2O_2$ dual-sensitive vesicles for enhanced glucose-responsive insulin delivery, Nano Lett. 17 (2) (2017) 733–739.
[19] J. Wang, Y. Ye, J. Yu, A.R. Kahkoska, X. Zhang, C. Wang, W. Sun, R.D. Corder, Z. Chen, S.A. Khan, J.B. Buse, Z. Gu, Core-Shell microneedle gel for self-regulated insulin delivery, ACS Nano 12 (3) (2018) 2466–2473.
[20] K. Podual, F.J. Doyle, N.A. Peppas, Glucose-sensitivity of glucose oxidase-containing cationic copolymer hydrogels having poly(ethylene glycol) grafts, J. Control. Release 67 (1) (2000) 9–17.
[21] K. Podual, F.J. Doyle, N.A. Peppas, Dynamic behavior of glucose oxidase-containing microparticles of poly(ethylene glycol)-grafted cationic hydrogels in an environment of changing pH, Biomaterials 21 (14) (2000) 1439–1450.
[22] A. Matsumoto, T. Ishii, J. Nishida, H. Matsumoto, K. Kataoka, Y. Miyahara, A synthetic approach toward a self-regulated insulin delivery system, Angew. Chem. Int. Ed. Eng. 51 (9) (2012) 2124–2128.
[23] A. Matsumoto, M. Tanaka, H. Matsumoto, K. Ochi, Y. Moro-Oka, H. Kuwata, H. Yamada, I. Shirakawa, T. Miyazawa, H. Ishii, K. Kataoka, Y. Ogawa, Y. Miyahara, T. Suganami, Synthetic "smart gel" provides glucose-responsive insulin delivery in diabetic mice, Sci. Adv. 3 (11) (2017) eaaq0723.
[24] L. Zhao, J. Ding, C. Xiao, X. Zhuang, X. Chen, Phenylboronic acid-functionalized polypeptide nanogel for glucose-responsive insulin release under physiological pH, J. Control. Release 213 (2015) e69.
[25] A. Matsumoto, R. Yoshida, K. Kataoka, Glucose-responsive polymer gel bearing phenylborate derivative as a glucose-sensing moiety operating at the physiological pH, Biomacromolecules 5 (3) (2004) 1038–1045.
[26] L. Liang, Z. Liu, A self-assembled molecular team of boronic acids at the gold surface for specific capture of cis-diol biomolecules at neutral pH, Chem. Commun. (Camb.) 47 (8) (2011) 2255–2257.
[27] D.H. Chou, M.J. Webber, B.C. Tang, A.B. Lin, L.S. Thapa, D. Deng, J.V. Truong, A. B. Cortinas, R. Langer, D.G. Anderson, Glucose-responsive insulin activity by covalent modification with aliphatic phenylboronic acid conjugates, Proc. Natl. Acad. Sci. USA 112 (8) (2015) 2401–2406.
[28] Y. Dong, W. Wang, O. Veiseh, E.A. Appel, K. Xue, M.J. Webber, B.C. Tang, X. W. Yang, G.C. Weir, R. Langer, D.G. Anderson, Injectable and glucose-responsive hydrogels based on Boronic acid-glucose complexation, Langmuir 32 (34) (2016) 8743–8747.
[29] W.L. Brooks, B.S. Sumerlin, Synthesis and applications of Boronic acid-containing polymers: from materials to medicine, Chem. Rev. 116 (3) (2016) 1375–1397.

[30] J. Yu, Y. Zhang, J. Wang, D. Wen, A.R. Kahkoska, J.B. Buse, Z. Gu, Glucose-responsive oral insulin delivery for postprandial glycemic regulation, Nano Res. 12 (7) (2019) 1539–1545.
[31] J. Wang, J. Yu, Y. Zhang, X. Zhang, A.R. Kahkoska, G. Chen, Z. Wang, W. Sun, L. Cai, Z. Chen, C. Qian, Q. Shen, A. Khademhosseini, J.B. Buse, Z. Gu, Charge-switchable polymeric complex for glucose-responsive insulin delivery in mice and pigs, Sci. Adv. 5 (7) (2019) eaaw4357.
[32] J. Yu, J. Wang, Y. Zhang, G. Chen, W. Mao, Y. Ye, A.R. Kahkoska, J.B. Buse, R. Langer, Z. Gu, Glucose-responsive insulin patch for the regulation of blood glucose in mice and minipigs, Nat. Biomed. Eng. 4 (5) (2020) 499–506.
[33] Y. Dong, W. Wang, O. Veiseh, E.A. Appel, K. Xue, M.J. Webber, B.C. Tang, X.-W. Yang, G.C. Weir, R. Langer, D.G. Anderson, Injectable and Glucose-Responsive Hydrogels Based on Boronic Acid–Glucose Complexation, Langmuir 32 (34) (2016) 8743–8747.
[34] Z. Ye, Y. Xiang, T. Monroe, S. Yu, P. Dong, S. Xian, M.J. Webber, Polymeric microneedle arrays with glucose-sensing dynamic-covalent bonding for insulin delivery, Biomacromolecules 23 (10) (2022) 4401–4411.
[35] S. Yu, W. Chen, G. Liu, B. Flores, E.L. DeWolf, B. Fan, Y. Xiang, M.J. Webber, Glucose-driven droplet formation in complexes of a supramolecular peptide and therapeutic protein, J. Am. Chem. Soc. 146 (11) (2024) 7498–7505.
[36] K. Ji, X. Wei, A.R. Kahkoska, J. Zhang, Y. Zhang, J. Xu, X. Wei, W. Liu, Y. Wang, Y. Yao, X. Huang, S. Mei, Y. Liu, S. Wang, Z. Zhao, Z. Lu, J. You, G. Xu, Y. Shen, J. B. Buse, J. Wang, Z. Gu, An orally administered glucose-responsive polymeric complex for high-efficiency and safe delivery of insulin in mice and pigs, Nat. Nanotechnol. 19 (12) (2024) 1880–1891.
[37] J. Xu, Y. Zhang, S. Zhao, J. Zhang, Y. Wang, W. Liu, K. Ji, G. Xu, P. Wen, X. Wei, S. Mei, L. Lu, Y. Yao, F. Liu, Y. Ma, J. You, J. Gao, J.B. Buse, J. Wang, Z. Gu, A bioinspired polymeric membrane-enclosed insulin crystal achieves long-term, self-regulated drug release for type 1 diabetes therapy, Nat. Nanotechnol. (2025), https://doi.org/10.1038/s41565-025-01860-0.
[38] C. Wang, Y. Ye, W. Sun, J. Yu, J. Wang, D.S. Lawrence, J.B. Buse, Z. Gu, Red blood cells for glucose-responsive insulin delivery, Adv. Mater. 29 (18) (2017) 1606617.
[39] Y. Xiao, H. Sun, J. Du, Sugar-breathing Glycopolymersomes for regulating glucose level, J. Am. Chem. Soc. 139 (22) (2017) 7640–7647.
[40] R. Yang, M. Wu, S. Lin, R.P. Nargund, X. Li, T. Kelly, L. Yan, G. Dai, Y. Qian, Q. Dallas-Yang, P.A. Fischer, Y. Cui, X. Shen, P. Huo, D.D. Feng, M.D. Erion, D. E. Kelley, J. Mu, A glucose-responsive insulin therapy protects animals against hypoglycemia. *JCI*, Insight 3 (1) (2018).
[41] M. Brownlee, A. Cerami, A glucose-controlled insulin-delivery system: semisynthetic insulin bound to lectin, Science 206 (4423) (1979) 1190–1191.
[42] N. Nakatsuka, K.A. Yang, J.M. Abendroth, K.M. Cheung, X. Xu, H. Yang, C. Zhao, B. Zhu, Y.S. Rim, Y. Yang, P.S. Weiss, M.N. Stojanović, A.M. Andrews, Aptamer-field-effect transistors overcome Debye length limitations for small-molecule sensing, Science 362 (6412) (2018) 319–324.
[43] R.A. Tromans, T.S. Carter, L. Chabanne, M.P. Crump, H. Li, J.V. Matlock, M. G. Orchard, A.P. Davis, A biomimetic receptor for glucose, Nat. Chem. 11 (1) (2019) 52–56.
[44] S. Xian, Y. Xiang, D. Liu, B. Fan, K. Mitrová, R.C. Ollier, B. Su, M.A. Alloosh, J. Jiráček, M. Sturek, M. Alloosh, M.J. Webber, Insulin-dendrimer Nanocomplex for multi-day glucose-responsive therapy in mice and swine, Adv. Mater. 36 (5) (2024) e2308965.
[45] P.D. Home, The pharmacokinetics and pharmacodynamics of rapid-acting insulin analogues and their clinical consequences, Diabetes Obes. Metab. 14 (9) (2012) 780–788.
[46] A. Lindholm, J. McEwen, A.P. Riis, Improved postprandial glycemic control with insulin aspart. A randomized double-blind cross-over trial in type 1 diabetes, Diabetes Care 22 (5) (1999) 801–805.
[47] J. Wang, Z. Wang, G. Chen, Y. Wang, T. Ci, H. Li, X. Liu, D. Zhou, A.R. Kahkoska, Z. Zhou, H. Meng, J.B. Buse, Z. Gu, Injectable biodegradable polymeric complex for glucose-responsive insulin delivery, ACS Nano 15 (3) (2021) 4294–4304.